

# Initial cell maturity changes following transplantation in a hyaluronan-based hydrogel and impacts therapeutic success in the stroke-injured rodent brain



Samantha L. Payne<sup>a,b</sup>, Anup Tuladhar<sup>b</sup>, Jaclyn M. Obermeyer<sup>a,b</sup>, Balazs V. Varga<sup>c</sup>, Carter J. Teal<sup>b</sup>, Cindi M. Morshead<sup>b,d,e</sup>, Andras Nagy<sup>f</sup>, Molly S. Shoichet<sup>a,b,g,\*</sup>

<sup>a</sup> Department of Chemical Engineering and Applied Chemistry, University of Toronto, Toronto, Ontario, M5S3E1, Canada

<sup>b</sup> Institute of Biomaterials and Biomedical Engineering, University of Toronto, Toronto, Ontario, M5S3E1, Canada

<sup>c</sup> Wellcome Trust Medical Research Council Cambridge Stem Cell Institute, University of Cambridge, Cambridge, UK

<sup>d</sup> Institute of Medical Science, University of Toronto, Toronto, Ontario, M5S3E1, Canada

<sup>e</sup> Department of Surgery, Division of Anatomy, University of Toronto, Toronto, Ontario, M5S3E1, Canada

<sup>f</sup> Lunenfeld-Tanenbaum Research Institute, Mount Sinai Hospital, Toronto, M5G1X5, Canada

<sup>g</sup> Department of Chemistry, University of Toronto, Toronto, Ontario, M5S3E1, Canada

## ARTICLE INFO

### Keywords:

Regeneration  
Cell transplantation  
Cell differentiation  
Cerebral cortex  
Neurons  
Stem cells

## ABSTRACT

Ischemic stroke results in a loss of neurons for which there are no available clinical strategies to stimulate regeneration. While preclinical studies have demonstrated that functional recovery can be obtained by transplanting an exogenous source of neural progenitors into the brain, it remains unknown at which stage of neuronal maturity cells will provide the most benefit. We investigated the role of neuronal maturity on cell survival, differentiation, and long-term sensorimotor recovery in stroke-injured rats using a population of human cortically-specified neuroepithelial progenitor cells (cNEPs) delivered in a biocompatible, bioresorbable hyaluronan/methylcellulose hydrogel. We demonstrate that transplantation of immature cNEPs result in the greatest tissue and functional repair, relative to transplantation of more mature neurons. The transplantation process itself resulted in the least cell death and phenotypic changes in the immature cNEPs, and the greatest acute cell death in the mature cells. The latter negatively impacted host tissue and negated any potential positive effects associated with cell maturity and the hydrogel vehicle, which itself showed some functional and tissue benefit. Moreover, we show that more mature cell populations are drastically altered during the transplantation process itself. The phenotype of the cells before and after transplantation had an enormous impact on their survival and the consequent tissue and behavioral response, emphasizing the importance of characterizing injected cells in transplantation studies more broadly.

## 1. Introduction

The ability of neural stem cell transplantation to restore brain function has been established in pre-clinical models of stroke [1–3] and has recently been tested in a Phase IIa clinical trial (PISCES-II); however, the optimal state of cell maturity for transplantation remains elusive. Neural progenitor cells (NPCs) derived from induced pluripotent stem cells (iPSCs) are an attractive source of cells for transplantation [1,4], but once transplanted these cells are influenced by the stroke microenvironment to differentiate into any neural progeny, and often predominantly become astrocytes [5,6], making it difficult to isolate the effect of neuronal delivery. It has been suggested that the use

of neuronal lineage-restricted precursors can both limit the differentiation into undesired cell types that can occur with the use of undifferentiated stem cells, and promote the formation of functional connections with the host tissue [7,8]. However, there are benefits and challenges with the use of both mature and undifferentiated cells for transplantation. More mature neurons may be better able to form functional synaptic connections with the host tissue, but are more susceptible to cell death during the transplantation process [9,10]. This cell death may be mitigated with the use of a hydrogel delivery system. Conversely, undifferentiated cells may be able to survive the transplantation process and secrete pro-survival factors into the host tissue, but may differentiate into an undesired cell type [11,12]. Although it

\* Corresponding author. Department of Chemical Engineering and Applied Chemistry, University of Toronto, Toronto, Ontario, M5S3E1, Canada.  
E-mail address: [molly.shoichet@utoronto.ca](mailto:molly.shoichet@utoronto.ca) (M.S. Shoichet).

<https://doi.org/10.1016/j.biomaterials.2018.11.020>

Received 15 August 2018; Received in revised form 31 October 2018; Accepted 12 November 2018

Available online 15 November 2018

0142-9612/ © 2018 Elsevier Ltd. All rights reserved.

has been suggested that differences in maturity may affect the ability of cells to survive the transplantation process [13], it is unknown specifically which cells are affected, and, most importantly, what effect this would have on the host tissue and functional outcome.

To test the effect of neuronal maturity on transplantation success in a rat model of stroke, we differentiated three populations of human induced-pluripotent stem cell (iPSC)-derived, cortically-specified, neuroepithelial progenitor cells (cNEPs) from a single starting population, into a neuronal population *in vitro* which has been previously described [13]. Identifying cNEPs along the differentiation continuum allows their maturity to be investigated in terms of transplantation success – that is, long-term cell survival and differentiation, as well as functional recovery of stroke-injured rats. Three cNEP populations of defined maturity were first compared *in vitro*: early-differentiated cells (0 days of *in vitro* differentiation), mid-differentiated cells (16 days of *in vitro* differentiation), and late differentiated cells (32 days of *in vitro* differentiation). The early-differentiated cells expressed Sox2 and nestin, the mid-differentiated cells expressed nestin, DCX, and  $\beta$ III-tubulin, and the late-differentiated cells primarily expressed  $\beta$ III-tubulin and MAP2. We delivered the early-, mid- and late-differentiated cells into the stroke injured brain in a hydrogel vehicle composed of hyaluronan (HA) and methylcellulose (MC), collectively termed HAMC, which has been shown to improve cell survival and distribution in several CNS pre-clinical models of disease [14–16]. HA has been shown to attenuate the inflammatory response, and to promote cell survival through a CD44-mediated mechanism, making it an attractive material for cell delivery. Moreover, HA is shear-thinning while MC is inverse thermal gelling, facilitating injectability and fast *in-situ* gelation.

Comparing the outcome of delivery of early, mid and late differentiated cells, we report that delivery of early cells, that is, the most immature, results in the greatest motor recovery. Interestingly, while we noted some positive effect of mid differentiated cells and HAMC alone on recovery, late differentiated cells showed no beneficial effect. Furthermore, we demonstrate that, despite initial differences in cell maturity *in vitro*, 50 days after delivery into the stroke-injured rat brain, all cell groups are remarkably similar in terms of survival and expression of stem, neuronal and glial cell markers. This suggests that there may be selective survival of subpopulations of transplanted cells, regardless of the phenotype of the starting population. We tested this hypothesis *in vitro*, finding that during cell harvesting, the detachment of cells and their subsequent injection through a fine gauge needle results in substantial death of mature neurons in the late-differentiated group specifically, despite encapsulation within the hydrogel. To the best of our knowledge, we are the first to demonstrate that the phenotypic composition of transplanted neural cells changes upon detachment from a culture plate and injection itself. The early differentiated population, which demonstrated minimal cell death and phenotype changes during transplantation, resulted in significantly improved behavioral recovery, whereas transplantation of the late differentiated population resulted in greater host tissue damage. Thus, mature cell death has significant consequences for tissue and functional outcomes after transplantation, which has broad implications for transplant applications.

## 2. Materials and methods

### 2.1. *In vitro* culture and differentiation of cNEPs

Culture, differentiation and characterization of cortically-specified neuroepithelial progenitor cells (cNEPs) has been previously described [13]. Briefly, cNEPs were obtained from a source of human fibroblasts reprogrammed into iPSCs and differentiated into neuroepithelial progenitor cells using a cocktail of small molecule inhibitors (unpublished results). Undifferentiated cNEPs were maintained in neural maintenance medium containing 50% DMEM-F12 with glutamine and HEPES, 50% Neurobasal, 0.1 mM 2-mercaptoethanol, 2 mM Glutamax,

1x N2 supplement, 0.05x B27 minus vitamin A supplement (Gibco), 20 ng/mL Insulin + zinc, 10 ng/ml FGF2, 3  $\mu$ M CHIR99021 (Peprotech), 10  $\mu$ M SB431542 (Peprotech), and 50 ng/ml noggin. Cells were routinely passaged with Accutase as single cells, and plated at  $3 \times 10^5$  cells per  $\text{cm}^2$  on a laminin coated surface. Cells were differentiated by culturing in serum-free medium containing 50% DMEM/F12 with glutamine and HEPES, 50% Neurobasal medium (Gibco), 0.1 mM 2-mercaptoethanol, 2 mM Glutamax, 1x N2 supplement, 0.05x B27 minus vitamin A supplement (Gibco), and 20 ng/mL Insulin + zinc for a defined number of days to obtain three stages of neuronal maturity: early, mid, and late. Early differentiated cells predominantly express sox2 and nestin, mid-differentiated cells express nestin, DCX, and  $\beta$ III-tubulin, and late-differentiated cells express DCX,  $\beta$ III-tubulin, and MAP2, while sox2 and nestin expression are absent.

### 2.2. HAMC preparation

A physical blend of hyaluronan (HA, 1200–1900 kDa, Novamatrix, Drammen, Norway) and methylcellulose (MC, 300 kDa, Shin-Etsu, Tokyo, Japan) was used to prepare HAMC, as previously described [13]. Briefly, 24 h before use, sterile filtered HA and MC were dissolved into artificial cerebrospinal fluid (aCSF) at a concentration of 1% w/v, mixed in a SpeedMixer (DAC 150 FVZ, Siemens) for 30 s and left at 4 °C overnight. Prior to use, HAMC was kept on ice for all experiments.

### 2.3. *In vitro* cNEP assays

Early, mid, or late-differentiated cNEPs were dissociated from the culture plate using Accutase (Sigma-Aldrich) and dissociated into a cell pellet. Cell were counted using Trypan blue exclusion and approximately 50,000 cells/ $\mu$ L were suspended in an equal volume of 1% w/v of each of HA and MC, resulting in a final concentration of 0.5% HA and 0.5% MC, w/v. 2  $\mu$ L of this solution was injected through a Hamilton 10  $\mu$ L Gastight syringe #1701 fitted with a 26G 45° beveled needle at a rate of 0.25  $\mu$ L/min into an Eppendorf tube and cell viability was determined. An additional 2  $\mu$ L of the cell-gel solution was removed from the sample prior to injection to determine cell viability after dissociation but without injection. In both instances cell viability was determined using calcein AM (for live cells) and ethidium homodimer (for dead cells, Thermo Fischer) and capturing images on an Olympus FV1000 laser scanning microscope. Cell viability was expressed as the percentage of live cells normalized to the initial cell number. Following injection, cells were diluted with differentiation medium and reseeded onto laminin-coated culture plates at a density of 30,000 cells/ $\text{cm}^2$  for immunocytochemistry.

### 2.4. *In vitro* cNEP immunocytochemistry

Either 1 h or 7 d after injection of cNEPs, media was removed and cells were fixed in 4% paraformaldehyde (PFA) for 20 min and washed twice in PBS. Cells were then blocked for 1 h with blocking solution (0.1% Triton-X-100, 5% BSA in PBS) and incubated with primary antibody diluted in blocking solution overnight at 4 °C. The following antibodies were used: anti-Sox2 (1:500, Abcam 137385); anti-DCX (1:500, Abcam ab18723); anti- $\beta$ -III tubulin (1:1000, Abcam ab41489); anti-MAP2 (1:500, Sigma Alrich m1406); anti-Ki67 (1:500, Abcam ab15580); anti-Caspase3 (1:500, Abcam ab13847). GFAP-positive astrocytes were not quantified following detachment and injection, because prior to 32 days of differentiation the number of cNEPs which differentiate into astrocytes is minimal. Cells were washed three times for 5 min each with PBS and incubated with the secondary antibodies diluted in blocking buffer for 2 h at room temperature. Alexa-tagged secondary antibodies (Molecular Probes, Invitrogen) were used at 1:500 dilutions: Alexa Fluor® 488 goat anti-rabbit IgG (Invitrogen, A11034), Alexa Fluor® 546 goat anti-mouse IgG (Invitrogen, A11003), and Alexa Fluor® 633 goat anti-chicken IgG (Invitrogen, A21103). Wells were

washed three times for 5 min each with PBS and left in PBS with DAPI for imaging. Images were captured on an Olympus FV1000 laser scanning microscope using a 20x objective lens and consistent settings between experimental groups. Protein expression was evaluated in 3 areas of each well to count cells and expressed as a percentage of total cells.

## 2.5. Animal procedures

Experimental procedures were performed in accordance with the Guide to the Care and Use of Experimental Animals and approved by the Animal Care Committee at the University of Toronto. Stroke surgeries were performed as described previously [13,17]. Seventy-five male Sprague-Dawley rats (Charles River) at 250 g were anaesthetized, the skull was shaved, and the skin cleaned and a rostral-caudal incision was made on the skull. Using sterile technique, the skull was exposed and three holes were drilled at coordinates: (1) AP 0.0, ML 3.0; (2) AP 2.3, ML 3.0, and (3) AP 0.7, ML 3.8. Animals were subjected to an endothelin-1 (Et-1, Calbiochem San Diego CA) induced stroke in the cortex and striatum by injecting 1  $\mu$ L of 400 pmol/ $\mu$ L Et-1 at a rate of 0.25  $\mu$ L/min through each of the drilled holes into the brain, 2.3 mm ventral from the surface of the skull for locations 1 and 2, and 7.0 mm ventral for location 3, using a 10  $\mu$ L Hamilton Gastight syringe (#1701) fitted with a 26G 45° beveled needle. The needle was left in place for 3 min after Et-1 injection and then slowly withdrawn to prevent backflow. The incision was sutured closed and animals were given Ketoprofen (3 mg/kg) and 3 mL saline for recovery. The functional deficit was assessed four days following injury using the staircase test and animals were evenly distributed into treatment groups for cell transplantation. Animals which had a minor deficit, i.e., their performance was equal to or greater than 80% of baseline on the staircase test, were excluded from behavioral analysis.

## 2.6. Behavioral task training and testing

The Montoya staircase and tapered beam tests were used to assess functional recovery of rats as previously described [18,19]. For the staircase test, rats were trained to retrieve pellets for 14 consecutive days, twice a day, and were required to obtain an average of at least 15 pellets per session to be considered successfully trained. For the tapered beam walk, rats were placed on the end of a tapered beam and trained for one day to cross the beam without interruption and enter a darkened goal box with a food reward. Baseline performance for each test was assessed by a blinded reviewer over three days immediately prior to the stroke surgery. At day 4 post-stroke, animals were tested to obtain a pre-transplantation measurement, and following cell transplantation, post-stroke animals were tested at 14, 28, 42, and 56 d on both tests. The staircase performance was recorded over 6 sessions (2 sessions per day for 3 days), and the final value was taken as an average of the last 4 sessions and expressed as a percentage of the individual animal's baseline performance. Animals without surviving cells at the terminal time point were removed from the final analysis. For the tapered beam test, a minimum of 5 runs across the beam was recorded for each animal during one session per testing period. A blind reviewer scored the number of hind limb foot faults that occurred during each run using the video playback, and the total number of foot faults was expressed as a percentage of the baseline performance.

## 2.7. Cell transplantation

The three populations of cells (early, mid, and late differentiated) were transplanted into the cortex of rats seven days after stroke surgery. Approximately 50,000 cells/ $\mu$ L were suspended in an equal volume of 1% HAMC, final concentration 0.5% HA/0.5% MC, w/v, and loaded into a Hamilton 10  $\mu$ L Gastight syringe #1701 fitted with a 26G 45° beveled needle. The needle tip was inserted 2.2 mm below the surface

of the skull and 2  $\mu$ L of cells in HAMC were injected into two of the three previously drilled locations corresponding to cortical lesion sites: AP 0.0 mm, ML 3.0 mm; and AP 2.3 mm, ML 3.0 mm. The rate of injection was 0.25  $\mu$ L/min and the needle was left in place for 3 min before being slowly withdrawn. Vehicle control animals were given an injection of 0.5% HA/0.5% MC w/v without cells. Cyclosporine A (CsA; Catalogue # C-6000, LC Laboratories, Woburn, MA, USA) was dissolved in conventional 65% ethanol, 35% Cremophor EL and rats received daily subcutaneous injections of CsA (15 mg/kg) for two days leading up to the cell transplantation. During the transplantation surgery, a subcutaneous osmotic minipump (Alzet, 2ML4) with CsA (15 mg/day) was implanted in all animals. Both incisions were sutured closed and animals were given ketoprofen (3 mg/kg) and saline for recovery. The researchers were blinded to which treatment each rat received.

## 2.8. Immunohistochemistry

At the terminal time point of 50 d post-transplantation, rats were sacrificed by CO<sub>2</sub> asphyxiation. Tissue was fixed by immersion in 4% PFA for 10 days followed by cryoprotection in 30% sucrose. Brains were flash frozen using dry ice cooled 2-methyl-butane and serially sectioned to 20  $\mu$ m using a cryostat (Leica CM3050S). Every sixth section from each brain was used for staining and quantification. The following antibodies were used for analysis: anti-human nuclear antigen (HuNu, 1:500, Millipore MAB1281); anti-Ki67 (1:500, Abcam ab15580); anti-DCX (1:500, Abcam ab18723); anti- $\beta$ -III tubulin (1:1000, Abcam ab41489); anti-NeuN (1:500, Abcam ab177587); anti-Caspase3 (1:500, Abcam ab13847); anti-gial fibrillary acidic protein (GFAP, 1:2000, DAKO Z0334); anti-human cytoplasm, STEM121 (1:1000, Takara Bio Y40410). Human nuclear antigen was chosen to identify cNEPs as it is a reliable and specific identifier of human cells in xenograft models and has been previously used by our group and others [13,38,48]. To investigate colocalization of cytoplasmic proteins with transplanted cNEPs, we used STEM121, which is present only in human cell cytoplasm [58]. Images were captured either using an Olympus FV1000 laser scanning microscope at 20x magnification to generate 25  $\mu$ m-thick z-stacks or using a Zeiss AxioScan.Z1 slide scanner at 10x magnification. Quantification was conducted by using Fiji is Just Image J (Rasband, W.S., ImageJ, U.S. National Institutes of Health, Bethesda, Maryland, USA, <http://imagej.nih.gov/ij/>, 1997–2016) and was conducted by a user blinded to treatment.

## 2.9. Tissue quantification

To calculate total cell number per brain, the number of HuNu-positive pixels in each stained section was counted, multiplied by the number of microns between sections sampled, and divided by the average number of pixels in one HuNu-positive cell to determine the number of cells per brain. To quantify cell fate, the number of either HuNu or STEM121-positive pixels was overlapped with positive pixels for each protein of interest to obtain the number of colocalized pixels. Protein expression was quantified as a fraction of colocalized pixels divided by total HuNu or STEM121 pixels to obtain a percentage value. To quantify the amount of caspase3, GFAP, NeuN,  $\beta$ III-tubulin and DCX expression in the host tissue, a region of interest (ROI) was selected to encompass all STEM121 + transplanted cells, and within this ROI the number of marker-positive/STEM121-negative pixels was quantified to represent host tissue adjacent to the transplant. The amount of caspase3 and GFAP in control groups containing no cells (Injury alone or HAMC) was quantified by selecting an ROI based on the NeuN-/DAPI+ lesion and using an in-house custom MATLAB script to quantify the number of positive pixels in a 100  $\mu$ m area surrounding the lesion, i.e., the perinfarct. Since quantification was conducted using different regions of interest in the cell vs non-cell groups, the data have been presented on different graphs.

## 2.10. Quantification of lesion volume

Sagittal tissue sections from 2.5 to 4.0 mm medial-lateral relative to the bregma were collected for lesion analysis. Sections stained for NeuN and counterstained with DAPI were used to quantify the lesion volume per brain as described elsewhere [16]. The lesion was defined as both the infarct and cavity; areas stained with DAPI but devoid of NeuN were defined as the infarct, whereas areas lacking in both DAPI and NeuN staining were defined as the cavity. Image J was used to manually trace the area of infarct and lesion for every sixth section of brain tissue. The lesion volume was calculated by summing the area of lesion for each representative tissue section and multiplying it by the thickness of the total tissue sample.

## 2.11. Statistical analysis

All data are reported as mean  $\pm$  standard error of the mean unless otherwise indicated. Statistical analysis was performed using GraphPad Prism 6 (GraphPad, La Jolla, CA). For comparisons between multiple groups, an analysis of variance (ANOVA) followed by Tukey's post-hoc test was used. For comparisons between two groups, a Student's t-test was used. A p-value of less than 0.05 (i.e., 95% confidence) was regarded as statistically significant (\* $p < 0.05$ , \*\* $p < 0.01$ , \*\*\* $p < 0.001$ ).

## 3. Results

### 3.1. Functional recovery observed in early-differentiated transplant animals

To determine an optimal cell maturity for transplantation we investigated three cell populations, based on differentiated neuronal maturity, for injection into the stroke-injured rat brain: early- (Sox2+, nestin+), mid- (nestin+, DCX+,  $\beta$ III-tubulin+) and late- ( $\beta$ III-tubulin+, MAP2+) differentiated cNEPs [13]. The time line for stroke injury, cell transplantation, and behavioral training and testing is outlined in Fig. 1A. To investigate the effect of transplanted cell maturity on animal behaviour, we used two sensorimotor assays: the staircase test [20] and the tapered beam test [21]. The staircase test showed differences in functional recovery (Fig. 1B–F) whereas the tapered beam test showed statistical differences neither between groups nor within each group (Fig. S1). At 4 d post-stroke and prior to cell injection, animals display an average deficit of approximately 50% of baseline performance in the staircase test. Compared to 4 d following stroke, animals transplanted with early-differentiated cells show significant improvement at both 42 and 56 d post-transplantation (Fig. 1B); animals transplanted with the mid-differentiated cells show significantly improved recovery at 56 d (Fig. 1C) and animals transplanted with the late cell group show no significant recovery over the course of the experiment (Fig. 1D). Interestingly, we also observed significant functional recovery in animals transplanted with the HAMC vehicle control at 56 d vs. 4 d post-stroke (Fig. 1E), demonstrating a beneficial effect of the vehicle itself and underlining its utility for cell delivery. However, even the recovery observed with HAMC was insufficient to overcome injury in the late-differentiated cell group, suggesting other host tissue effects resulted from transplantation of these more mature cells. We observed no evidence of significant recovery in the injury alone group at any time point tested (Fig. 1F). Thus, we observed significant differences over time with transplantation of early- and mid-differentiated cells and with HAMC, but no significant differences between the groups (Fig. 1G).

### 3.2. cNEPs survive and proliferate in all maturity groups

We next examined the survival and proliferation of transplanted cells by immunostaining the tissue for human nuclear antigen (HuNu) to detect human cells within the rat brain (for survival) and then those co-localized with Ki67 (for proliferation) (Fig. 2A–L). We detected

HuNu+ nuclei in the cortex at the approximate injected location for early- (Fig. 2A–D), mid- (Fig. 2E–H) and late-differentiated cells (Fig. 2I–L) at 50 d after transplantation. We found that approximately 80% of animals that received transplants contain surviving cells, which was similar across all experimental groups (Fig. 2M), and that the average number of cells per brain does not differ significantly, largely due to the high variability in the mid- and late-differentiated groups (Fig. 2N); however, there is a trend towards more cells in the mid- and late-differentiated cell groups vs. the early-differentiated group (and this difference would be significant at 90% confidence with  $p = 0.086$  for mid- vs. early-differentiated cells; and  $p = 0.088$  for late- vs. early-cells). Given that approximately  $2 \times 10^5$  cells were transplanted into each animal, the early-differentiated group has  $28 \pm 10.4\%$  of the initial cell number whereas the mid- and late differentiated cell groups have  $206 \pm 67.0\%$ , and  $202 \pm 54.8\%$ , respectively. Although on average more cells are found in the mid- and late-differentiated groups, there are no significant differences in the percentage of proliferating cells between groups at the terminal time point (Fig. 2O).

### 3.3. Expression of phenotype markers did not differ between transplant groups

We next investigated the expression of phenotype markers to determine if the pre-transplantation maturity of the cell populations is maintained post-transplantation, or if cells differentiate further *in vivo*. Markers examined included: the neural stem cell marker, Sox2, neuronal lineage markers DCX (neuroblasts),  $\beta$ III-tubulin (immature neurons), and NeuN (mature neurons), and the astrocyte marker GFAP. Surprisingly, and in contrast to what is observed pre-transplantation, there are no significant differences between cell maturation markers comparing brains from early-, mid- and late-differentiated cell groups at 50 d after transplantation (Fig. 3A–E). On average per brain, 5% of cells expressed Sox2, 30% expressed DCX, 25% expressed  $\beta$ III-tubulin, 5% expressed NeuN, and 20% expressed GFAP, indicating that the majority of transplanted cells adopt an immature neuronal or glial phenotype at 50 d post-transplantation.

### 3.4. Detachment & injection through syringe causes acute cell death and loss of mature phenotype

To gain a greater understanding of any changes that may be occurring to the cells during the transplantation process, we re-examined our cells *in vitro* using the identical protocol for cells being transplanted *in vivo* – that is, cell detachment from culture plates followed by injection through an identical needle at the same rate (0.25  $\mu$ L/min). We hypothesized that the transplantation paradigm affects mature cell survival, leading to a change in the population phenotype. We tested our hypothesis by detaching and injecting all three cell phenotypes (early-, mid-, and late-differentiated) separately through a 26-gauge needle and immunostaining the cells for markers of cell maturity after either 1 h or 7 d in culture. Following detachment and injection, cell viability decreases in all three groups whereas following detachment alone, cell viability decreases significantly only in the late cell group relative to the viability of adhered cells (Fig. 4A). Viability for early- and mid-differentiated cells following injection is approximately 85% compared to  $\sim 50\%$  in the late-differentiated group, relative to the adhered cell viability. Investigating phenotype, we observed that 1 h following either detachment alone or detachment and injection, the early-differentiated cells (Fig. 4B) express similar levels of Sox2, DCX,  $\beta$ III-tubulin and MAP2 as adherent cells, demonstrating that early-differentiated cells do not change significantly during processing and injection. In contrast, compared to the adherent levels, the mid- (Fig. 4C) and late- (Fig. 4D) differentiated cells have significantly reduced levels of DCX and  $\beta$ III-tubulin following detachment and injection, and no MAP2 expression – a protein expression pattern that differs considerably overall from adherent cultures. These changes in phenotype

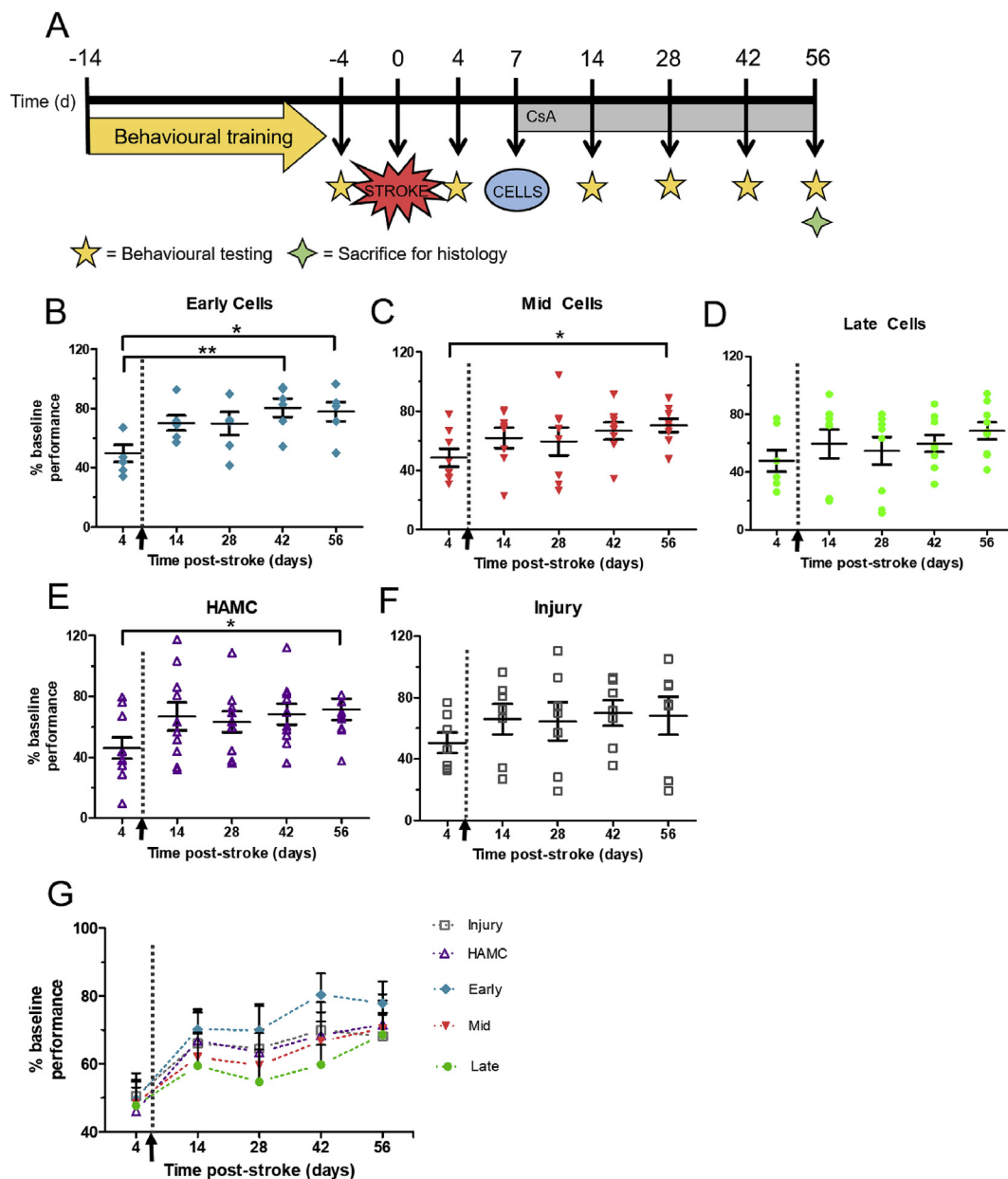


**Fig. 1.** Paradigm for cell transplantation and behavioral analysis of functional recovery using the Montoya staircase test. (a) Animals were trained on the behavioral tests for two weeks prior to stroke surgeries and performance baselines were established 4 d before endothelin-1 stroke. Animals were implanted with a cyclosporin A (CsA) osmotic pump at the time of cell transplantation. Early-, mid- or late-differentiated cNEPs were injected into the stroke-injured brain 7 d following a stroke injury. Following cell injection, performance was measured biweekly for 56 d. Animals were sacrificed 56 d after injury. Within-group differences were assessed relative to the injury time point (4 d post stroke) for (b) early-differentiated, (c) mid-differentiated, (d) late-differentiated cells, (e) HAMC, and (f) injury alone. Animals injected with the early-differentiated cells improved significantly at 42 d (\*\*p < 0.01) and 56 d (\*p < 0.05) relative to pre-cell injection values at 4 d whereas those injected with the mid-differentiated cells and HAMC improved significantly (\*p < 0.05) at 56 d. Injury alone groups showed no significant improvement. (g) There were no significant differences between experimental groups. Dotted line with arrow delineates time of cell transplantation. (n = 6–10, Mean ± SEM, one-way ANOVA with repeated measures and Tukey's post hoc, \*p < 0.05, \*\*p < 0.01).

are accompanied by a change in cell morphology in the late-differentiated group, wherein the long neuronal processes are not re-established *in vitro* (Fig. 4E), even when cultures are maintained for longer time periods of 7 d post-injection (Fig. S2). These results demonstrate that the transplantation paradigm causes acute cell death, leading to changes in phenotype and viability of the more mature transplanted cells.

### 3.5. Host injury and gliosis are increased with transplantation of late-differentiated, mature cells

To gain insight into the effect of the transplanted cells on the host brain tissue, we quantified lesion volume, apoptosis and gliosis. The lesion is comprised of an infarct and cavity and was measured by immunostaining the host brain tissue for NeuN+ neurons and DAPI + cells. The infarct volume is defined as the region of DAPI+/NeuN- cells and cavity as the DAPI-/NeuN- region (Fig. 5A). The infarct volume is significantly greater in those brains transplanted with late-differentiated cells vs. mid-differentiated cells, HAMC, or injury alone

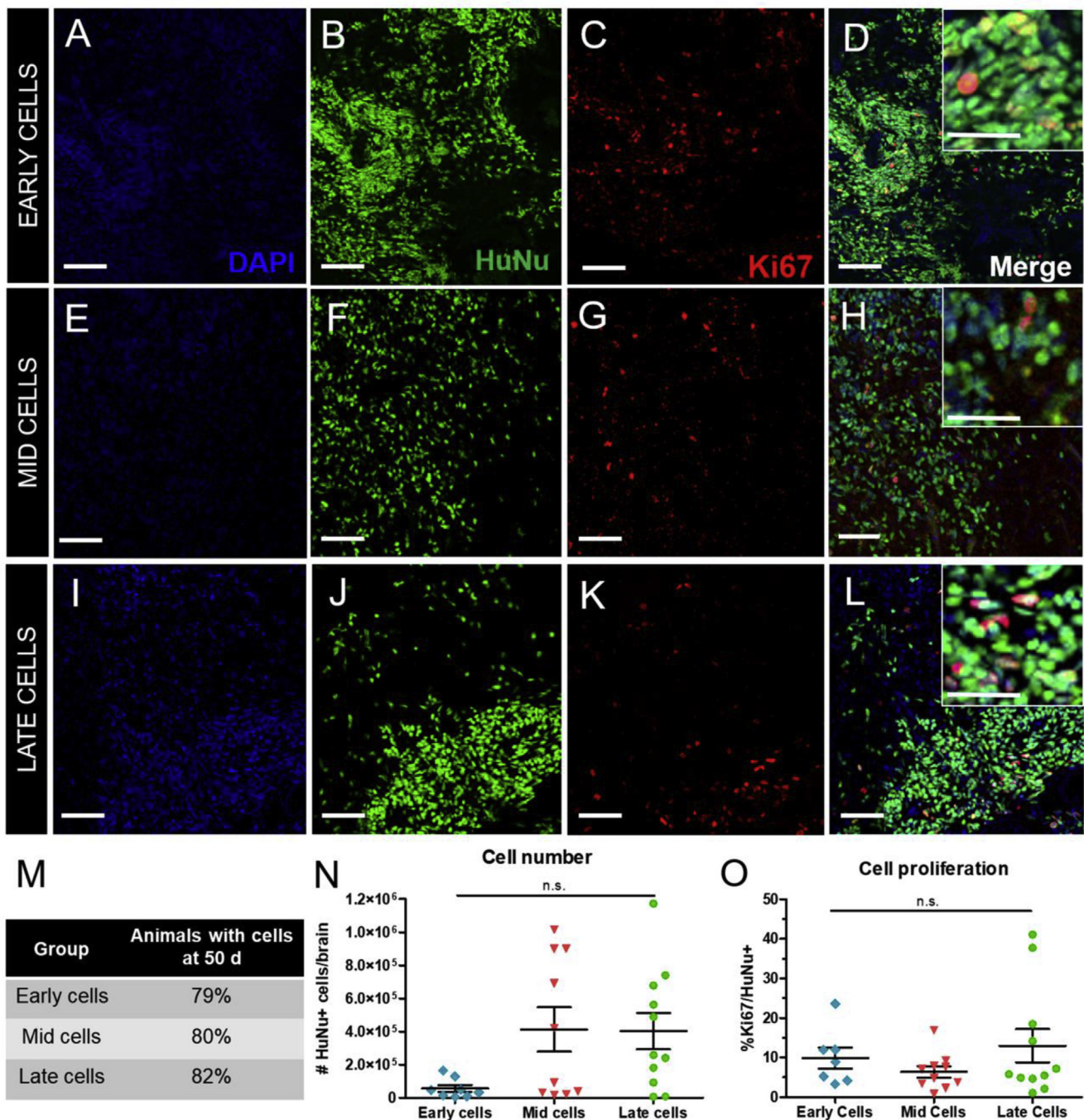
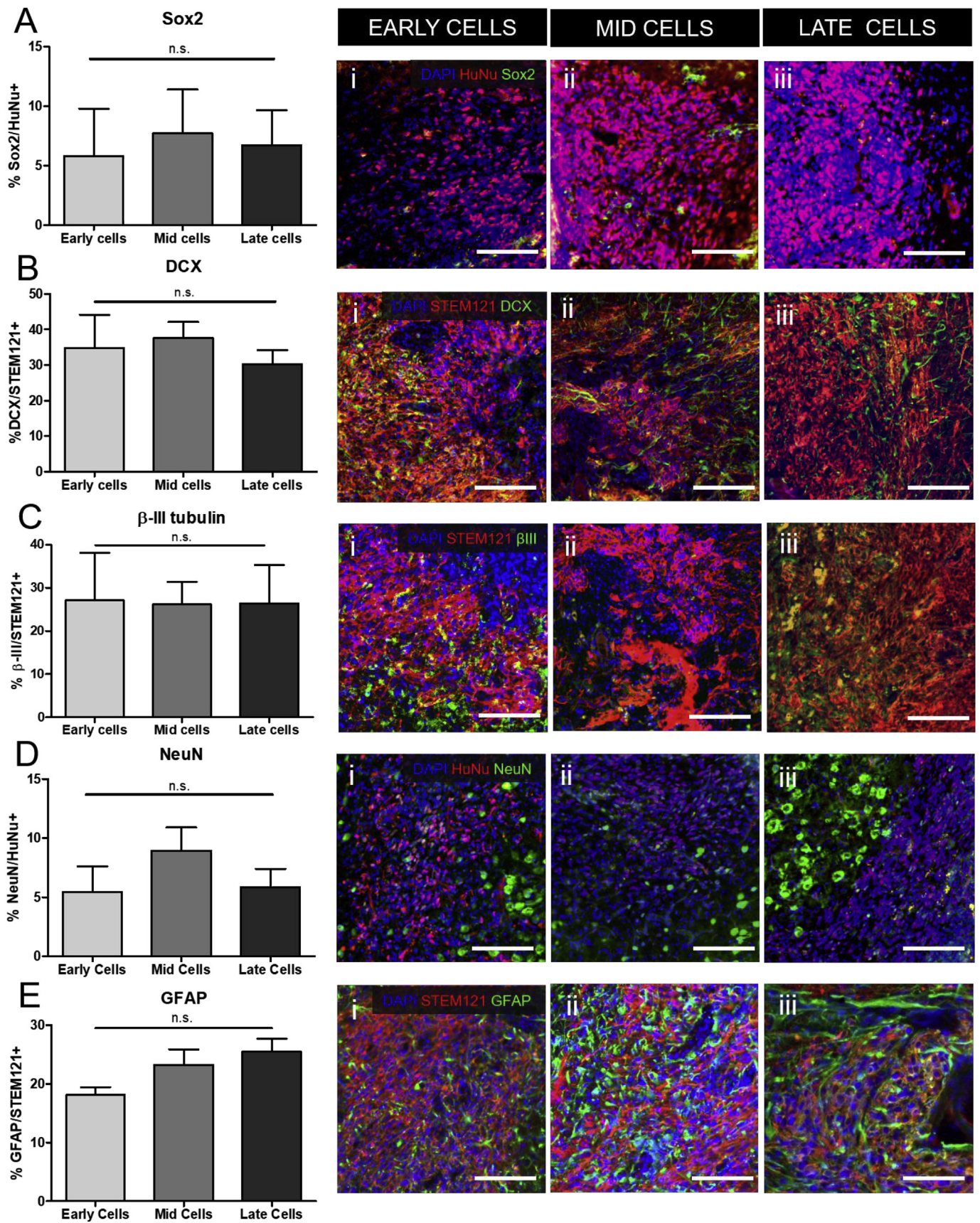


**Fig. 2.** Cell survival and proliferation 50 d post-transplantation. (a–l) Representative immunohistological images of cNEPs stained for nuclei (DAPI, blue), human nuclear antigen (HuNu; green) and Ki67 (red). (m) The number of animals with cells detected at the terminal time point for each maturity type transplanted. (n) Quantification of average HuNu + cell number per brain. (o) Quantification of the average percentage of proliferating cNEPs as determined by colocalization of HuNu and Ki67. Scale bar = 100  $\mu$ m. Inset scale bar = 50  $\mu$ m n = 8–10, mean  $\pm$  SEM, one-way ANOVA with Tukey's post hoc, \*p  $\leq$  0.05. (For interpretation of the references to colour in this figure legend, the reader is referred to the Web version of this article.)

(Fig. 5B). While animals transplanted with the late-differentiated cells have the largest cavity volume, it does not differ significantly between groups (Fig. 5C). The total lesion volume is significantly greater in the late-differentiated group compared to the mid-differentiated cell group (Fig. 5D).

The impact of the transplanted cells on apoptosis and gliosis in the host brain was quantified immediately adjacent to the transplanted cells by Caspase3 (Fig. 6A) and GFAP expression (Fig. 6B), respectively. To differentiate between host and transplanted cells, the tissue was also stained with STEM121, a human cytoplasmic marker. There is

significantly more apoptosis in the peri-infarct host tissue in animals injected with late-differentiated cells than early-differentiated cell transplants, as demonstrated by Caspase3 + /STEM121-cells (Fig. 6D). There is also a trend towards increased transplant cell apoptosis with increased cell maturity (from early-to mid-to late-), but no significant differences using Caspase3 + /STEM121 + staining (Fig. 6C). To better understand the glial host tissue response, we compared GFAP + /STEM121-staining in the host brain tissue among the three transplanted cell groups. Host tissue gliosis adjacent to the transplant is significantly higher in animals transplanted with the late differentiated



(caption on next page)

**Fig. 3.** Histological analysis of cell phenotype in the stroke-injured brain at 50 d after transplantation. Quantification of number of pixels positive for each marker per brain revealed no significant difference in protein expression after transplantation among the (i) early-, (ii) mid-, and (iii) late-differentiated cell groups in terms of (a) Sox2 for neural stem cells; (b) doublecortin (DCX) for neuroblasts; (c)  $\beta$ III-tubulin for immature neurons; (d) NeuN for mature neurons; and (e) GFAP for glial cells. Mean + SEM,  $n = 6-8$ , one-way ANOVA with Tukey's post hoc test,  $p \leq 0.05$ . Scale bar = 100  $\mu\text{m}$ . (Nuclei were stained with DAPI, blue; transplanted cells were stained with HuNu or STEM121, red; each marker, Sox2, DCX,  $\beta$ III, NeuN, and GFAP, green). (For interpretation of the references to colour in this figure legend, the reader is referred to the Web version of this article.)

cell group compared to the early- or mid-differentiated groups (Fig. 6E). Interestingly, the amount of host caspase3 and GFAP expression was also evaluated in the peri-infarct region of brains from the injury and HAMC control groups, and it was found that animals injected with HAMC alone had significantly less caspase3 expression than the injury control group (Fig. S3), demonstrating a positive tissue effect of the vehicle itself which may explain the functional benefits observed. We also quantified the amount of NeuN+,  $\beta$ III-tubulin+, and DCX+ host in the vicinity of the transplanted cNEPs (Fig. 6F–H), and found that, while there was no difference in the number of  $\beta$ III-tubulin or DCX pixels between cell groups, there were significantly more NeuN+ pixels in the early-compared to the late-differentiated group. Together, these results demonstrate that transplantation of the more mature cell population has a negative effect on the host tissue in terms of increased lesion volume, cell death, and gliosis that negated the beneficial effects of HAMC alone.

#### 4. Discussion

To determine the effect of neuronal progenitor cell maturity on transplant success, we delivered human early-, mid- and late-differentiated cNEPs in a HAMC hydrogel into the stroke-injured rat brain, finding the fastest behavioral recovery with the transplantation of early-differentiated cNEPs. Importantly, our cells were derived from the same starting population, making them directly comparable in terms of maturity without the confounding factor of different sources. Despite clear differences in cell phenotype *in vitro*, we observed similar cell proliferation, and expression profiles of neural stem and progenitor markers across groups after 50 days *in vivo*. We investigated cell viability and phenotype following the injection process and determined that injection causes selective death of mature neurons, leading to an increase in the number of dead cells delivered into the brain in the late-differentiated group. Fig. 7 summarizes the differences in cell survival and functional repair as a function of cell maturity. This injection of dead cells leads to negative host tissue effects and inhibited the beneficial effects of HAMC alone on both behavioral recovery and host tissue death, emphasizing a need to characterize changes in cell viability and phenotype post-injection.

When we investigated cell phenotype and survival *in vitro* after cell detachment and injection through a syringe needle, we found that mature cells in the late-differentiated group underwent significant death likely due to their greater fragility and disruption of cell processes during detachment from the culture plate. Surprisingly, the interplay between cell maturity and transplantation paradigm has not been previously reported and cell survival alone is rarely reported or quantified. Viability of human NSCs or NPCs immediately following injection has been reported as between 81% in saline [22] and 97% in a hydrogel for the clinically-tested CTX cell line [23], and as low as 60% in saline for mouse NPCs [24]. There are limited data for transplantation of more differentiated progeny; however, one study investigating the use of mesencephalic dopaminergic neuron precursors noted that more differentiated precursors had poor cell viability following fluorescent activated cell sorting (FACS) and transplantation into the brain compared to less-differentiated progeny [10]. Another study investigating undifferentiated or differentiated striatal human NSCs found no difference in viability after cell harvesting, but also found no differences in cell survival or functional outcome after transplantation into a mouse model of Huntington's Disease [25]. GFAP-positive astrocytes were not

quantified following detachment and injection, because, prior to 32 days of differentiation the number of cNEPs which differentiate into astrocytes is minimal. A number of factors such as cell processing, injection rate, concentration of cells, needle gauge and length, time that cells remain in the syringe before injection, and delivery vehicle all contribute to acute cell viability [26,27]. The damage to adherent, late-differentiated cells during the detachment and pelleting process is difficult to avoid, but other parameters can be investigated to reduce cell death in this group. For example, the HAMC hydrogel delivery vehicle used herein could co-deliver pro-survival or differentiation factors to promote the survival of more mature cells and/or direct their differentiation [16,28].

Interestingly, animals transplanted with HAMC alone showed both behavioral recovery at 56 days whereas injury alone animals did not, and reduced caspase3 expression relative to those animals with injury alone. These data demonstrate that HAMC promotes host tissue repair and is thus a good cell delivery vehicle. Although HAMC is resorbed and cleared from tissue in approximately 3–7 days [15,29], host cells may infiltrate into HAMC and contribute to early tissue preservation and the recovery seen; however, given that we characterized the tissue at 50 days after HAMC injection, it is difficult to confirm this hypothesis. Others have reported host cell infiltration into non-degradable or slowly resorbable materials, such as ECM [30] and electrospun agarose/methylcellulose hydrogels [31], at late time points (84 and 60 days, respectively), and Ghurman et al. report cell infiltration as early as 24 h following implantation of the hydrogel [30]. We too have observed cell migration with HAMC injection into the spinal cord [32]; however, in that case HAMC was modified with both cell adhesive RGD peptides and the PDGF growth factor whereas in the current study there was no additional modification to HAMC. Previous studies have shown HAMC to promote cell survival through a CD44-HA mediated interaction [14] and anti-inflammatory properties; here we show its beneficial effects on host tissue in terms of reduced apoptosis and on behaviour, which has not been previously observed. It is possible that an early reduction in inflammation leads to a decrease in long-term cell apoptosis through a CD44-dependent modulation of pro-inflammatory cytokine secretion in leukocytes [33]. Future studies beyond the scope of this manuscript will be needed to investigate this further and link the decrease in host cell apoptosis to the functional recovery observed.

In addition to the importance of investigating the changes in cell viability following injection, determining the impact of these changes on the host tissue is also essential. We demonstrated that the increased cell death observed in the late-differentiated group led to greater host tissue damage than that observed with early- and mid-differentiated cell transplants, as evidenced by the greater lesion volume, gliosis at the site of injection and greater caspase3 expression. This corroborates the only other study on the effect of cell viability on host brain tissue where dead cells that were purposefully injected into the brain resulted in an increased inflammatory response and a larger lesion [34]. Lesion volume, depending on the location, has been correlated with the degree of impairment in preclinical stroke models [22,35] while cortical atrophy has been correlated with worsening staircase test performance [8]. The inflammatory response following a stroke is important for tissue repair but can also lead to long-term negative effects. Initial infiltration of immune cells into the lesion can help to remove debris caused by dying cells, but also results in secretion of pro-inflammatory factors leading to inflammation and gliosis. Others have shown that the inflammatory response is decreased by 14 days following a stroke and diminishes at



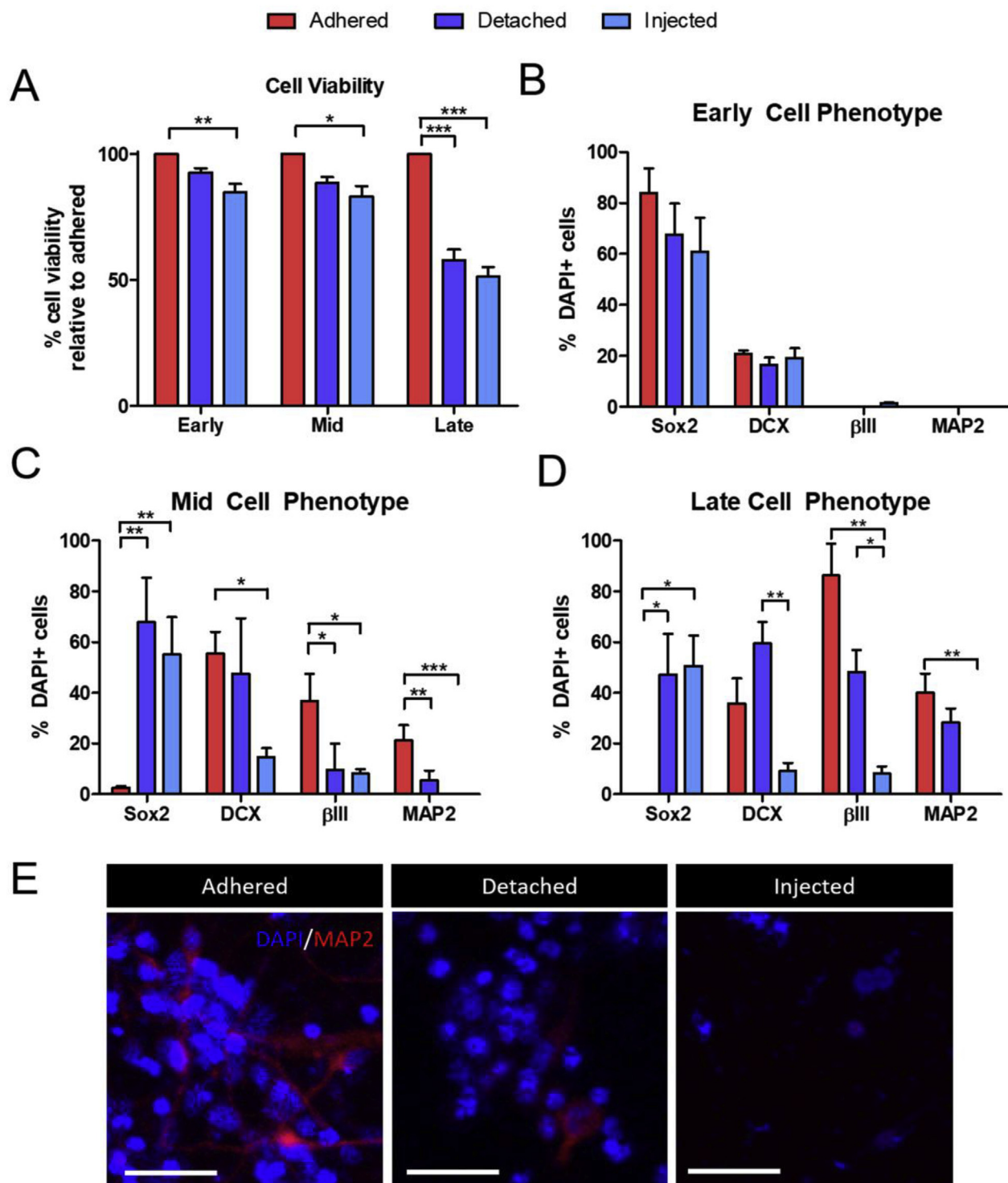


**Fig. 4.** Quantification of cNEP viability and phenotype following *in vitro* injection and cell culture. Cells were cultured following detachment alone or detachment and injection through a 26-gauge needle and either assayed using a live/dead stain or immunolabeled for neural stem cells (Sox2), immature neurons (DCX;  $\beta$ III-tubulin), and mature neurons (MAP2). (a) Cell viability decreases significantly following injection for all groups and significantly following detachment for only the late-differentiated group. (b) Early-differentiated cells maintain their Sox2 expression following injection whereas (c) mid- and (d) late-differentiated cells lose their mature neuronal phenotype following injection. Adhered = cultured cells; Detached = after detachment from culture plate, but before injection; Injection = after both detachment and injection. (e) Representative images of late-differentiated cell morphology labeled with anti-MAP2 (red) before and after detachment and/or syringe injection. Mean + SEM, One-way ANOVA with Tukey's post hoc, \* $p < 0.05$ , \*\* $p < 0.01$ , \*\*\* $p < 0.001$ ,  $n = 5$ . Scale bar = 50  $\mu$ m. (For interpretation of the references to colour in this figure legend, the reader is referred to the Web version of this article.)

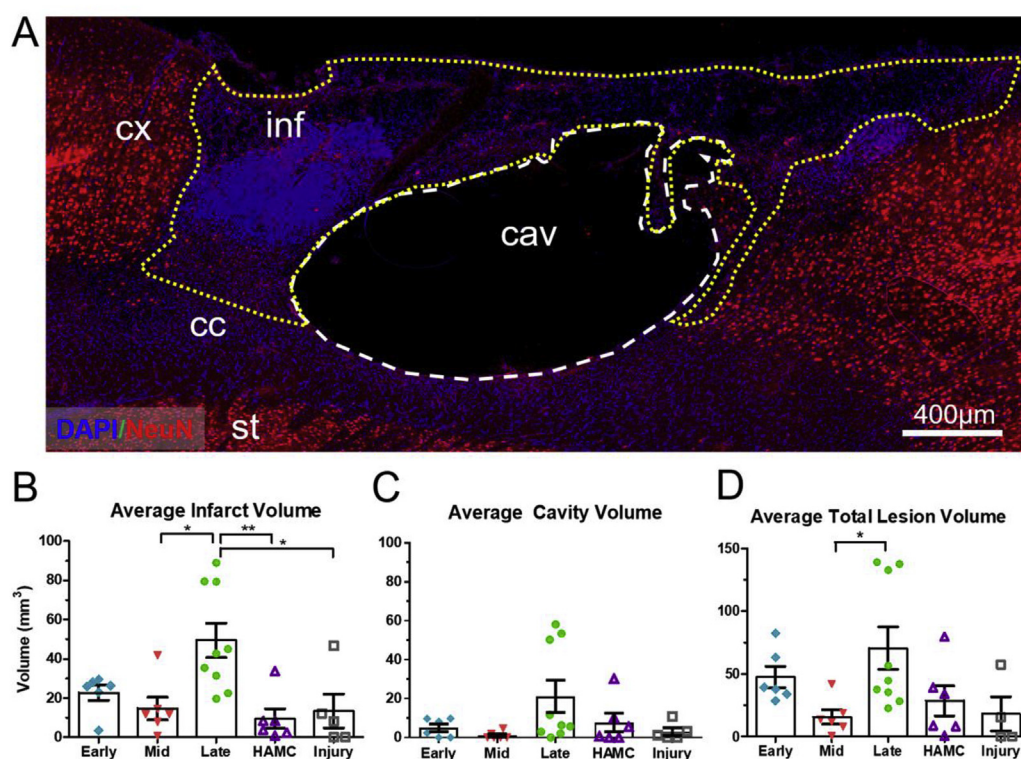


**Fig. 5.** Lesion volume 50 d after transplantation of cNEPs. (a) A representative image from the late-differentiated group. Lesion volume is defined as sum of infarct volume (volume of DAPI+/NeuN- tissue) and cavity volume (volume of DAPI-/NeuN-tissue). DAPI = blue, NeuN = red. cav = cavity, cc = corpus callosum, cx = cortex, inf = infarct, st = striatum. Quantification of volume of (b) infarct, (c) cavity, and (d) total lesion (= infarct + cavity). Mean  $\pm$  SEM,  $n = 6-9$  per group, One-way ANOVA with Tukey's post hoc, \* $p < 0.05$ , \*\* $p < 0.01$ . (For interpretation of the references to colour in this figure legend, the reader is referred to the Web version of this article.)

later time points [36,37] and therefore differences would likely be undetectable at 56 days post-stroke in our tissue. Apoptosis of transplanted cells is rarely reported at time points greater than one week; however, in one study, 25% of total transplanted cells were positive for caspase3 at 8 weeks post-transplantation [38], which is consistent with our data. In our study, animals transplanted with the late-differentiated cells showed the greatest amount of gliosis in the host tissue adjacent to the transplant site. The glial scar, which forms in response to injury in the peri-infarct tissue to limit damage, also acts as a chronic barrier that prevents axon regeneration in the brain [39,40]. The size of the glial scar has been correlated with reduced functional recovery [41], which is consistent with our data. Interestingly, there appears to be a threshold of cell death that must be reached before there is a measurable impact on host tissue and behaviour; while the mid-differentiated group had some mature neuron death, it did not result in the detrimental host tissue effects found with the late-differentiated group, suggesting that only when cell viability decreases beyond a certain threshold does it impact the host.

The death of more mature cells at the onset of transplantation is likely responsible for the observed similarities in cell phenotype at the terminal time point *in vivo*, as the remaining progenitor cells proliferated and differentiated. In a previous study of cNEP survival 7 days post-transplantation, differences in number and phenotype based on cell maturity were observed *in vivo*.<sup>13</sup> Together with the data presented herein, where no difference in phenotype was observed at 50 days post-transplantation, these results suggest that both the transplantation process and the microenvironment in the brain impact cells and that they evolve over time during engraftment. Minimal NeuN expression and evidence of proliferation in our transplants suggest that most neurons present in all groups were relatively immature at this terminal time point, despite the fact that, at 32 days of differentiation *in vitro*, a significant proportion of cNEPs were phenotypically mature [13]. Our data are consistent with other studies that show NPCs differentiated for 21 days prior to transplantation had more than double the initial number of cells 1 month after transplantation, reflecting significant proliferation [42]. In another study, NPCs that were analyzed at 50

weeks after transplantation expressed immature and proliferation markers, Sox2 and Ki67, respectively, in the brain and exhibited a 20-fold increase in the number of transplanted cells [43].

Although our data show that the injection paradigm was responsible for acute changes in phenotype, it is well documented that the microenvironment of the brain contributes over time to the fate of transplanted cells. Others have reported that transplant location into the spinal cord influences the maturity of iPSC-derived NPCs [44], and that the injured brain microenvironment favours the differentiation to astrocytes over neurons when an undifferentiated NSC population is transplanted [6,14,45]. Since the population of cells that survived the injection process were of a less-differentiated phenotype, their fate was likely influenced by the stroke microenvironment, as evidenced by the higher expression of GFAP *in vivo* (20–30%) than is typically seen in cNEPs differentiated in culture for 30 days (15% *in vitro*) (Varga et al., in preparation) and the lower expression of  $\beta$ III-tubulin *in vivo* (25%) compared to that *in vitro* (80%) [13]. Others have seen this so-called “phenotypic fluidity” [46] after transplantation even when cells are pre-differentiated towards a neuronal lineage and sorted using PSA-NCAM, a marker of migrating neuroblasts [16,47,48]. It is possible that even with commitment to a neuronal lineage, if cells are not terminally differentiated, they may switch to a glial fate. The increase in GFAP-positive cells *in vivo* at 50 days, relative to that *in vitro* at 32 days, may also reflect the longer time required to differentiate astrocytes, which typically follow that of neurons [49].

We observed that the transplantation of late-differentiated cells results in acute loss of mature cell viability and provides no functional benefit. Others that have investigated transplantation of cells of varying maturity status reported mixed outcomes. Jensen et al., observed a similar trend to our data where no differences in cell survival or phenotype of iPSC-NPCs were observed between transplanted cells of different maturity status after one month *in vivo* [50]. Fricker-Gates et al. demonstrated decreased survival when post-natal neurons were transplanted compared to less differentiated, embryonic progenitors [12]. Interestingly, they also showed that embryonic stage neuroblasts or immature neurons could form synaptic connections with the host while

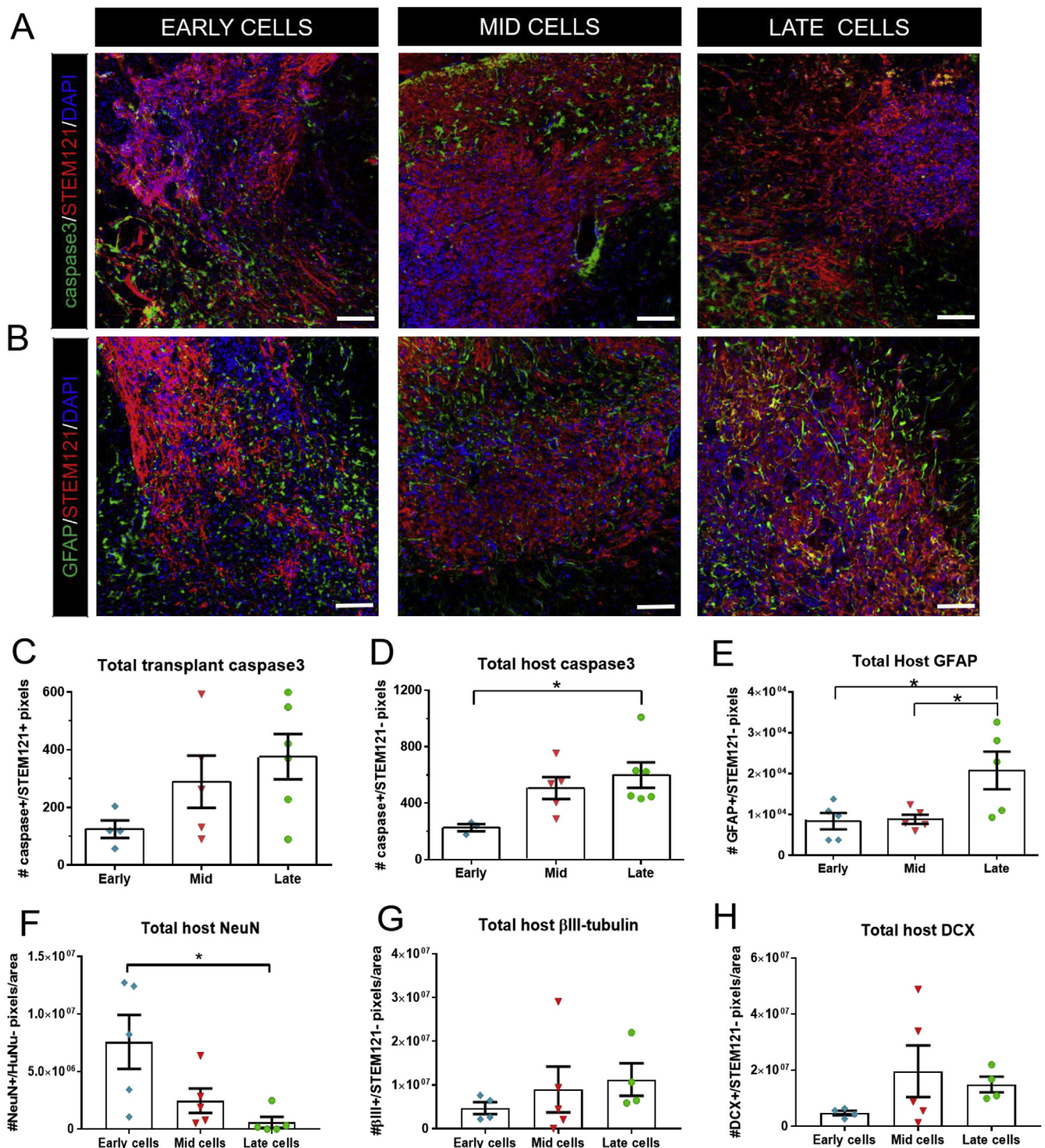


**Fig. 6.** Host and transplant cell death and changes in host tissue composition 50 d after injection of cNEPs. Representative images of (a) caspase3 (apoptotic cells, green) and (b) GFAP (astrocytes, green) immunostaining for each transplanted maturity co-localized with STEM121 (human cells, red) and DAPI (nuclei, blue). Quantification of cell death via total caspase3 expression in (c) transplant tissue (caspase3+/STEM121+) or (d) host tissue (caspase3+/STEM121-). (e) Quantification of host GFAP (GFAP+/STEM121-), (f) Quantification of host NeuN (NeuN+/HuNu-), (g) Quantification of host betaIII-tubulin (betaIII-tubulin+/STEM121-), and (h) Quantification of host DCX (DCX+/STEM121-). Mean  $\pm$  SEM,  $n = 4-8$  per group, One-way ANOVA with Tukey's post hoc, \* $p < 0.05$ , \*\* $p < 0.01$ . Scale bar = 100  $\mu$ m. (For interpretation of the references to colour in this figure legend, the reader is referred to the Web version of this article.)

post-natal projection neurons did not. While our findings are consistent with those of Jensen and Fricker-Gates, we recognize that they contradict other studies, making the ideal maturity status difficult to identify. For example, rats transplanted with 'cortically-fated' human NPCs had greater recovery than 'unfated' NPCs [11] while pre-differentiated GABAergic neurons maintained their phenotype *in vivo* and

exhibited better survival than undifferentiated NSCs [6]. Abeyasinghe et al. hypothesized that undifferentiated transplanted cells predominantly became astrocytes that contributed to the glial scar whereas the pre-differentiated GABAergic neurons increased endogenous neurogenesis [6]. Several factors may account for these differing results: susceptibility to cell death during the injection paradigm, model of

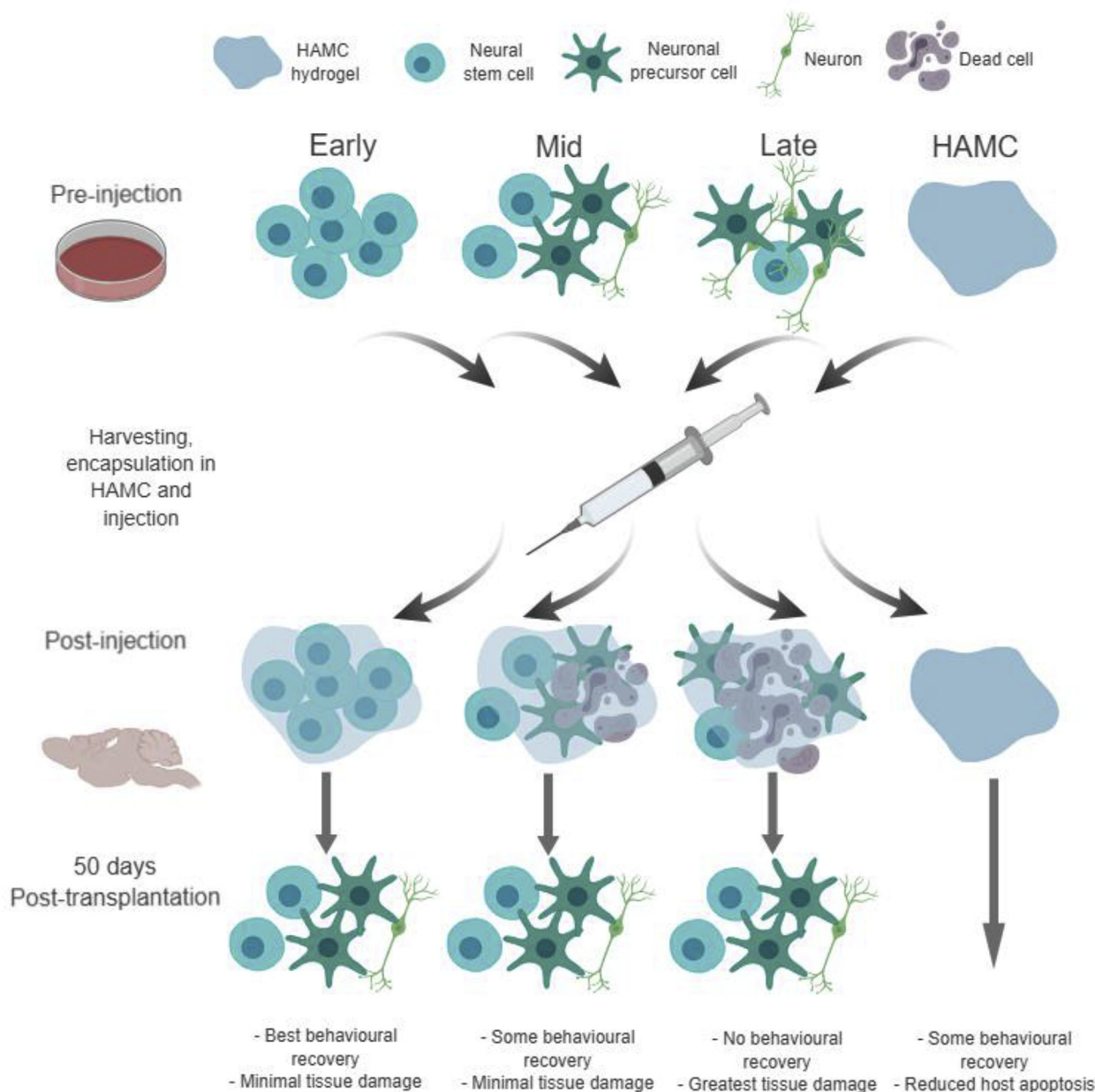


**Fig. 7.** Schematic summarizing the impact of harvesting and injecting cells of different in vitro maturity on tissue and functional repair in a rat model of stroke. Initially early, mid, and late-differentiated cNEP populations are phenotypically distinct in terms of maturity. Following harvesting, encapsulation in HAMC and injection, mature cells are selectively killed, leading to the delivery of more dead cells in the mid and late-differentiated groups than the early-differentiated group. Post-transplantation, at 50 days, cell populations are phenotypically similar due to the acute death of mature cells, leading to increased host tissue damage. While the HAMC hydrogel itself showed functional and tissue benefit, it was insufficient to overcome the effects of the mature cell group.

injury, anatomical location of transplantation, and the neuronal subtype of the cells, which could affect their ability to respond and adapt to the stroke microenvironment [7,12,51]. For example, differentiation of NSCs into functionally mature midbrain dopaminergic neurons has been shown to confer a resistance to the excitatory cytotoxicity that can be found in the post-stroke microenvironment that less mature cells do not possess [9].

We observed on average more cells present in the mid- and late-differentiated groups than the early-differentiated group, which was only significant at 90% confidence. In addition, the animals with the greatest number of cells also had the highest proportion of Ki67+ proliferating cells. One possible explanation for this is a mechanism known as the ‘Phoenix Rising’ pathway. Following an injury in endogenous regenerative models (e.g., newts, xenopus tadpoles, and

mouse digit tips) cells undergoing apoptosis will induce proliferation of nearby stem cells. This mechanism is thought to be an essential step in initiating successful regeneration [52,53]. In the murine digit tip this phenomenon is mediated by caspase3 expression in apoptotic cells, which induces prostaglandin-2 secretion in neighboring stem cells and upregulates proliferation [54]. We demonstrated that there was significantly more caspase3 expression in the host tissue surrounding the cNEPs, and a trend towards increased expression in the transplanted cells in the late-differentiated group. Although more work is required to determine if this mechanism can affect cNEP proliferation, it suggests that the transplantation of more dead cells in the late-differentiated cell group may have led to an increase in proliferation of the remaining live cells, resulting in similar numbers of cells at the terminal time point, regardless of starting number of live cells.

Our results indicate that more immature cNEPs, that is the early-differentiated cell group, are best suited for transplantation success. The early-differentiated cell group exhibited the earliest within-group recovery with the staircase tests, although, curiously, with the lowest average number of cells at day 50 after transplantation. There were no differences between groups in the beam test, although this may reflect the greater sensitivity of the staircase test to this sensorimotor injury model [55]. Others have observed that cell number is not necessarily correlated with recovery [22] and that the paracrine signaling by transplanted cells can be more important than the cells themselves for recovery [3]. Our phenotype analysis indicated that there were very few mature neurons present at day 50 post-transplant, so it is unlikely that the recovery that we observed was due to functional integration with the host circuitry. In addition, the time frame in which we saw recovery is too early for the extensive axonal growth and electrophysiological maturity others report with human cells [8,43,56]. For these reasons, host-transplant functional connectivity was not pursued. Instead, early-differentiated cells may secrete pro-survival factors that have paracrine effects on host tissue and thus cell integration may not be required for tissue and behavioral repair. Indeed, we observed that there were more NeuN+ host neurons in the area of the transplanted cNEPs in the early-compared to the late-differentiated group, suggesting that early differentiated cells promoted host neuron survival. This constitutes an active debate about whether transplantation of neurons is necessary to promote recovery. On the one hand, paracrine effects seem to be sufficient [3] and on the other hand, functional connections between host and transplant may be important [57]. Herein, pre-differentiation of cells was detrimental due to the associated cell death on their transplantation and thus had no functional benefit, suggesting that paracrine effects were most important to the repair observed.

## 5. Conclusions

We investigated the effect of cell maturity on transplantation success and found that undifferentiated progenitor cells resulted in the greatest and fastest functional repair. In contrast, injection of the late-differentiated cell group caused greater tissue damage due to acute cell death during the transplantation process itself and consequently resulted in no functional repair. The cell delivery vehicle, HAMC, induced recovery at the terminal time point, but even this recovery was inhibited when combined with the late-differentiated cells. This highlights the importance of both the delivery vehicle, where reduced host tissue damage was also observed relative to injury alone, and the impact of the transplantation process itself on cell fate.

## Declaration of conflicting interests

The authors have no conflicts to disclose; however, we acknowledge an issued patent on cell delivery in HAMC.

## Acknowledgments

We are grateful for funding from: the Canada First Research Excellence Fund to Medicine by Design at the University of Toronto (to MSS, CMM, AN), the Canadian Institutes of Health Research (Foundation grant to MSS, Operating grant to CMM) and the Natural Sciences and Engineering Research Council (CGS-D to SLP). We thank Elliott Birman and Julia Luo for assistance with tissue processing and members of the Shoichet lab for thoughtful discussions and review.

## Appendix A. Supplementary data

Supplementary data related to this article can be found at <https://doi.org/10.1016/j.biomaterials.2018.11.020>.

## References

- [1] K. Oki, et al., Human-induced pluripotent stem cells form functional neurons and improve recovery after grafting in stroke-damaged brain, *Stem Cell*. 30 (2012) 1120–1133.
- [2] J. Lam, et al., Delivery of iPSC-NPCs to the stroke cavity within a hyaluronic acid matrix promotes the differentiation of transplanted cells, *Adv. Funct. Mater.* 24 (44) (2014) 7053–7062.
- [3] I.H. Lee, et al., Delayed epidural transplantation of human induced pluripotent stem cell-derived neural progenitors enhances functional recovery after stroke, *Sci. Rep.* 7 (2017) 1943.
- [4] T. Yuan, et al., Human induced pluripotent stem cell-derived neural stem cells survive, migrate, differentiate, and improve neurologic function in a rat model of middle cerebral artery occlusion, *Stem Cell Res. Ther.* 4 (3) (2013) 73.
- [5] G. Dziejczapolski, et al., Survival and differentiation of adult rat-derived neural progenitor cells transplanted to the striatum of hemiparkinsonian rats, *Exp. Neurol.* 183 (2) (2003) 653–664.
- [6] H.C.S. Aboysinghe, et al., Pre-differentiation of human neural stem cells into GABAergic neurons prior to transplant results in greater repopulation of the damaged brain and accelerates functional recovery after transient ischemic stroke, *Stem Cell Res. Ther.* 6 (1) (2015) 1–19.
- [7] A.C. Lepore, et al., Differential fate of multipotent and lineage-restricted neural precursors following transplantation into the adult CNS, *Neuron Glia Biol.* 1 (02) (2004) 113–126.
- [8] F.A. Soma, et al., Peptide-based scaffolds support human cortical progenitor graft integration to reduce atrophy and promote functional repair in a model of stroke, *Cell Rep.* 20 (8) (2017) 1964–1977.
- [9] B. Watmuff, C.W. Pouton, J.M. Haynes, In vitro maturation of dopaminergic neurons derived from mouse embryonic stem cells: implications for transplantation, *PLoS One* 7 (2) (2012) e31999.
- [10] M.E. Jönsson, et al., Identification of transplantable dopamine neuron precursors at different stages of midbrain neurogenesis, *Exp. Neurol.* 219 (1) (2009) 341–354.
- [11] D. Tornero, et al., Human induced pluripotent stem cell-derived cortical neurons integrate in stroke-injured cortex and improve functional recovery, *Brain* 136 (Pt 12) (2013) 3561–3577.
- [12] R.A. Fricker-Gates, et al., Late-stage immature neocortical neurons reconstruct interhemispheric connections and form synaptic contacts with increased efficiency in adult mouse cortex undergoing targeted neurodegeneration, *J. Neurosci.* 22 (10) (2002) 4045–4056.
- [13] S.L. Payne, et al., In vitro maturation of human iPSC-derived neuroepithelial cells influences transplant survival in the stroke-injured rat brain, *Tissue Eng.* 24 (3–4) (2018) 351–360.
- [14] Brian G. Ballios, et al., A hyaluronan-based injectable hydrogel improves the survival and integration of stem cell progeny following transplantation, *Stem Cell Rep.* 4 (6) (2015) 1031–1045.
- [15] B.G. Ballios, et al., A hydrogel-based stem cell delivery system to treat retinal degenerative diseases, *Biomaterials* 31 (9) (2010) 2555–2564.
- [16] T. Führmann, et al., Injectable hydrogel promotes early survival of induced pluripotent stem cell-derived oligodendrocytes and attenuates long-term teratoma formation in a spinal cord injury model, *Biomaterials* 83 (2016) 23–36.
- [17] A. Tuladhar, C.M. Morshead, M.S. Shoichet, Circumventing the blood–brain barrier: local delivery of cyclosporin A stimulates stem cells in stroke-injured rat brain, *J. Contr. Release* 215 (2015) 1–11.
- [18] M.G. Balkaya, et al., Behavioral outcome measures to improve experimental stroke research, *Behav. Brain Res.* 352 (2018) 161–171.
- [19] M. Ragas, D. Nagarajan, A.M. Corbett, Refining forelimb asymmetry analysis: correlation with Montoya staircase contralateral function post-stroke, *J. Neurosci. Methods* 290 (2017) 52–56.
- [20] C.P. Montoya, et al., The “staircase test”: a measure of independent forelimb reaching and grasping abilities in rats, *J. Neurosci. Methods* 36 (2) (1991) 219–228.
- [21] T. Schallert, M. Woodlee, S. Fleming, Disentangling multiple types of recovery from brain injury, *Pharmacol. Cereb. Ischemia* 2002 (2002) 216.
- [22] E.J. Smith, et al., Implantation site and lesion topology determine efficacy of a human neural stem cell line in a rat model of chronic stroke, *Stem Cell*. 30 (4) (2012) 785–796.
- [23] P. Moshayedi, et al., Systematic optimization of an engineered hydrogel allows for selective control of human neural stem cell survival and differentiation after transplantation in the stroke brain, *Biomaterials* 105 (2016) 145–155.
- [24] B.A. Aguado, et al., Improving viability of stem cells during syringe needle flow through the design of hydrogel cell carriers, *Tissue Eng.* 18 (2012) 7–8.
- [25] G. El-Akabay, et al., Implantation of undifferentiated and pre-differentiated human neural stem cells in the R6/2 transgenic mouse model of Huntington's disease, *BMC Neurosci.* 13 (2012) 97.
- [26] T. Rossetti, F. Nicholls, M. Modo, Intracerebral cell implantation: preparation and characterization of cell suspensions, *Cell Transplant.* 25 (4) (2016) 645–664.
- [27] A. Tuladhar, S.L. Payne, M.S. Shoichet, Harnessing the potential of biomaterials for brain repair after stroke, *Front. Mater.* 5 (2018) 14.
- [28] A.J. Mothe, et al., Repair of the injured spinal cord by transplantation of neural stem cells in a hyaluronan-based hydrogel, *Biomaterials* 34 (15) (2013) 3775–3783.
- [29] J.W. Austin, et al., The effects of intrathecal injection of a hyaluronan-based hydrogel on inflammation, scarring and neurobehavioural outcomes in a rat model of severe spinal cord injury associated with arachnoiditis, *Biomaterials* 33 (18) (2012) 4555–4564.
- [30] H. Ghuman, et al., Long-term retention of ECM hydrogel after implantation into a sub-acute stroke cavity reduces lesion volume, *Acta Biomater.* 63 (2017) 50–63.

- [31] C.J. Rivet, et al., Cell infiltration into a 3D electrospun fiber and hydrogel hybrid scaffold implanted in the brain, *Biomater* 5 (1) (2015) e1005527.
- [32] T. Führmann, et al., Combined delivery of chondroitinase ABC and human induced pluripotent stem cell-derived neuroepithelial cells promote tissue repair in an animal model of spinal cord injury, *Biomed. Mater.* 13 (2) (2018) 024103.
- [33] S. Ruppert, et al., Tissue integrity signals communicated by high-molecular weight hyaluronan and the resolution of inflammation, *Immunol. Res.* 58 (2–3) (2014) 186–192.
- [34] M. Modo, et al., Effects of implantation site of dead stem cells in rats with stroke damage, *Neuroreport* 14 (1) (2003) 39–42.
- [35] E. Irlé, An analysis of the correlation of lesion size, localization and behavioral effects in 283 published studies of cortical and subcortical lesions in old-world monkeys, *Brain Res. Rev.* 15 (3) (1990) 181–213.
- [36] D. Ito, et al., Enhanced expression of Iba1, ionized calcium-binding adapter molecule 1, after transient focal cerebral ischemia in rat brain, *Stroke* 32 (5) (2001) 1208–1215.
- [37] X. Hu, et al., Microglia/macrophage polarization dynamics reveal novel mechanism of injury expansion after focal cerebral ischemia, *Stroke* 43 (11) (2012) 3063–3070.
- [38] K. Jin, et al., Transplantation of human neural precursor cells in matrigel scaffolding improves outcome from focal cerebral ischemia after delayed posts ischemic treatment in rats, *J. Cerebr. Blood Flow Metabol.* 30 (3) (2009) 534–544.
- [39] Y. Li, et al., Gliosis and brain remodeling after treatment of stroke in rats with marrow stromal cells, *Glia* 49 (3) (2005) 407–417.
- [40] L. Huang, et al., Glial scar formation occurs in the human brain after ischemic stroke, *Int. J. Med. Sci.* 11 (4) (2014) 344–348.
- [41] I. Badan, et al., Accelerated glial reactivity to stroke in aged rats correlates with reduced functional recovery, *J. Cerebr. Blood Flow Metabol.* 23 (7) (2003) 845–854.
- [42] M.B. Jensen, et al., Survival and differentiation of transplanted neural stem cells derived from human induced pluripotent stem cells in a rat stroke model, *J. Stroke Cerebrovasc. Dis.* 22 (4) (2013) 304–308.
- [43] J.C. Niclis, et al., Long-distance axonal growth and protracted functional maturation of neurons derived from human induced pluripotent stem cells after intracerebral transplantation, *Stem Cells Transl. Med.* 6 (6) (2017) 1547–1556.
- [44] K. Sugai, et al., Pathological classification of human iPSC-derived neural stem/progenitor cells towards safety assessment of transplantation therapy for CNS diseases, *Mol. Brain* 9 (1) (2016) 85.
- [45] A.J. Joannides, et al., Environmental signals regulate lineage choice and temporal maturation of neural stem cells from human embryonic stem cells, *Brain* 130 (5) (2007) 1263–1275.
- [46] E.D. Laywell, et al., Neuron-to-astrocyte transition: phenotypic fluidity and the formation of hybrid asteroles in differentiating neurospheres, *J. Comp. Neurol.* 493 (3) (2005) 321–333.
- [47] J.M. Fortin, et al., Transplantation of defined populations of differentiated human neural stem cell progeny, *Sci. Rep.* 6 (2016) 23579.
- [48] T. Führmann, et al., Combined delivery of chondroitinase ABC and human induced pluripotent stem cell-derived neuroepithelial cells promote tissue repair in an animal model of spinal cord injury, *Biomed. Mater.* 13 (2018) 024103.
- [49] C. Dehay, H. Kennedy, Cell-cycle control and cortical development, *Nat. Rev. Neurosci.* 8 (2007) 438.
- [50] M.B. Jensen, et al., Effects of neural differentiation maturity status of human induced pluripotent stem cells prior to grafting in a subcortical ischemic stroke model, *Neurol. Psychiatr. Brain Res.* 22 (3–4) (2016) 178–182.
- [51] V.L. Sheen, et al., Neural precursor differentiation following transplantation into neocortex is dependent on intrinsic developmental state and receptor competence, *Exp. Neurol.* 158 (1999) 47–62.
- [52] F. Li, et al., Apoptotic cells activate the “phoenix rising” pathway to promote wound healing and tissue regeneration, *Sci. Signal.* 3 (110) (2010) ra13.
- [53] J. Beom, et al., Concurrent use of granulocyte-colony stimulating factor with repetitive transcranial magnetic stimulation did not enhance recovery of function in the early subacute stroke in rats, *Neurol. Sci.* 36 (5) (2015) 771–777.
- [54] A.-S. Tseng, et al., Apoptosis is required during early stages of tail regeneration in *Xenopus laevis*, *Dev. Biol.* 301 (1) (2007) 62–69.
- [55] K.L. Schaar, M.M. Brenneman, S.I. Savitz, Functional assessments in the rodent stroke model, *Exp. Transl. Stroke Med.* 2 (1) (2010) 13.
- [56] P. Lu, et al., Prolonged human neural stem cell maturation supports recovery in injured rodent CNS, *J. Clin. Invest.* 127 (9) (2017) 3287–3299.
- [57] D. Tornero, et al., Synaptic inputs from stroke-injured brain to grafted human stem cell-derived neurons activated by sensory stimuli, *Brain* 140 (3) (2017) 692–706.
- [58] S. Kelly, T.M. Bliss, A.K. Shah, G.H. Sun, M. Ma, W.C. Foo, J. Masel, M.A. Yenari, I.L. Weissman, N. Uchida, T. Palmer, G.K. Steinberg, Transplanted human fetal neural stem cells survive, migrate, and differentiate in ischemic rat cerebral cortex, *Proc. Natl. Acad. Sci. U. S. A.* 101 (2004) 11839–11844.